

ChemComm

Accepted Manuscript



This is an *Accepted Manuscript*, which has been through the Royal Society of Chemistry peer review process and has been accepted for publication.

Accepted Manuscripts are published online shortly after acceptance, before technical editing, formatting and proof reading. Using this free service, authors can make their results available to the community, in citable form, before we publish the edited article. We will replace this *Accepted Manuscript* with the edited and formatted *Advance Article* as soon as it is available.

You can find more information about *Accepted Manuscripts* in the [Information for Authors](#).

Please note that technical editing may introduce minor changes to the text and/or graphics, which may alter content. The journal's standard [Terms & Conditions](#) and the [Ethical guidelines](#) still apply. In no event shall the Royal Society of Chemistry be held responsible for any errors or omissions in this *Accepted Manuscript* or any consequences arising from the use of any information it contains.

COMMUNICATION

Integrated, highly crystalline and water stable coordination framework film on various substrates and water-assisted protonic conductivity

Cite this: DOI: 10.1039/x0xx00000x

Received 00th January 2012,
Accepted 00th January 2012Chen Xiao,^{a,b} Zhengyu Chu,^b Xiao-Ming Ren,^{*a,b} Tian-Yu Chen^{a,b} and Wanqin Jin^{*a}

DOI: 10.1039/x0xx00000x

www.rsc.org/

The integrated, highly crystalline and water stable Prussian blue analogues film were successfully fabricated on the porous α -Al₂O₃, the conducting ITO and the flexible non-woven fabrics substrates, respectively, using the self-assembly approach. The proton conduction was investigated for both powdered pellet and the film on the porous α -Al₂O₃ substrate. This study promotes the practical applications of MOFs-based proton conductors in various devices.

Solid-state protonic conductors are of prime interest, being expected as the appealing application of electrolytes in sensors and fuel cells.¹⁻³ Typical proton conducting materials are amorphous organic polymers with nanosized water channels, such as the extensively studied Nafion,⁴ or crystalline inorganic compounds such as perovskite-type oxides (ceramic oxides)⁵ and phosphate,⁶ and both are widely used in fuel cell technology. Nafion-like polymers are efficient at temperatures below 100 °C whereas ceramic oxides operate at temperatures higher than 600 °C. These known materials do not cover the intermediate temperature range (200-500 °C) with satisfactory proton conductivity.³

In this context, it is notable that the recent burgeoning research is focusing on proton-conducting metal-organic frameworks (MOFs) or coordination polymers (CP) with pores or channels.⁷⁻¹² MOFs-based materials are considered as intermediate proton conductors between these two extremes because they have channels, as do the organic polymers, but also show crystalline nature, as do the oxides. Up to date, most studies focus on the protonic conduction of powders, and seldom reports on the protonic conductivity of membrane/film of MOFs-based materials. However, from the viewpoint of practical application, it is the most important aim to fabricating and investigating the protonic conducting membrane/film of MOFs-based materials because the proton exchange membranes/films have only being used in various devices.

Prussian blue analogues (PBAs) are a family of coordination frameworks. The zeolitic water molecules and ligand water molecules form a three-dimensional (3-D) hydrogen-bonding network in the cubic lattice of PBAs. The intrinsic structure property

offers the excellent opportunities of PBAs as proton conducting materials. Herein, we present our study on the fabrication of integrated, highly crystalline and water stable PBA films on various substrates using self-assembly approach and their proton conduction behaviours.

The polycrystalline sample of PBAs, Cu₃[Co(CN)₆]₂·nH₂O, was synthesized according to the previously reported procedure,^{13,14} and its cubic phase was confirmed by powder X-ray diffraction (PXRD) technique. The PXRD patterns measured at ambient temperature are shown in Fig. S1 in ESI for the as-prepared sample and that immersed in water for two months, the PXRD patterns of two samples are in agreement well with that of cubic Cu₃[Co(CN)₆]₂·nH₂O.^{13,14} It is worth mentioning that the sample immersed in water for two months shows almost the same sharp diffraction peaks by comparison of the as-prepared sample, indicating that the cubic Cu₃[Co(CN)₆]₂·nH₂O is water stable.

The Cu₃[Co(CN)₆]₂·nH₂O crystalline film was tried to grow on different kinds of substrates by self-assembly strategy since the proton conductor is used in the form of thin-film or membrane for the practical application in fuel cells or other devices. The integrated and high crystalline Cu₃[Co(CN)₆]₂·nH₂O films were successfully achieved on the porous α -alumina, the conducting indium-tin oxide (ITO) and the flexible non-woven fabrics (which is made of polyvinylidene fluoride, abbr. as PVDF; and the SEM photo is shown in ESI) substrates using the layer-by-layer self-assembly approach, respectively. The thickness of Cu₃[Co(CN)₆]₂·nH₂O film is controllable by means of tuning the cycle numbers of layer-by-layer self-assembly, and the details are provided in ESI.

Figs. 1a-1d show sequentially the SEM images of the surface of porous α -alumina substrate, the Cu₃[Co(CN)₆]₂·nH₂O film at different magnifications and the cross section of film on α -alumina substrate, respectively. It clearly showed that the micrometer-size crystals are accumulated to form a continuous film on the surface of the porous α -alumina substrate, and the thin film thickness of Cu₃[Co(CN)₆]₂·nH₂O is about 2 μ m and the crystalline phase of film verified by PXRD analysis (Fig. 1e) is consistent with the powder sample and take the homogeneous pure phase. Figs. 1f and 1g display the SEM images of Cu₃[Co(CN)₆]₂·nH₂O grown on the

conducting ITO and the flexible non-woven fabrics substrates, respectively. On the surfaces of such different nature substrates, the submicrometer-size and closed-spaced cubic crystals formed the integrated and uniform films.

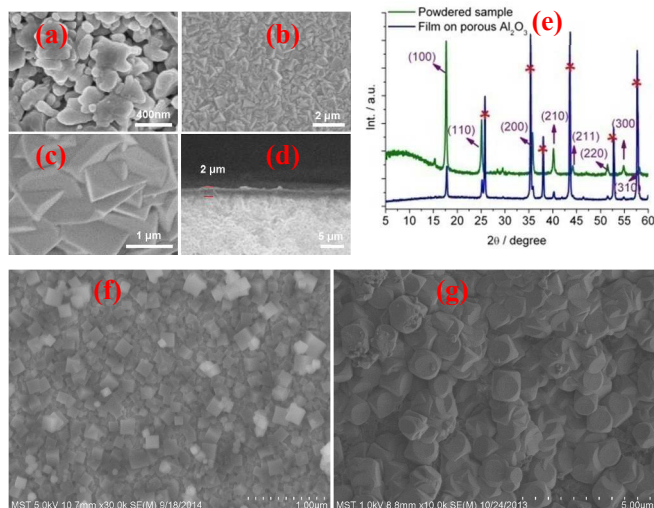


Fig. 1 SEM images of (a) pure porous α -alumina substrate (b, c) $\text{Cu}_3[\text{Co}(\text{CN})_6]_2 \cdot n\text{H}_2\text{O}$ film at different magnifications and (d) cross section of $\text{Cu}_3[\text{Co}(\text{CN})_6]_2 \cdot n\text{H}_2\text{O}$ film on porous α -alumina substrate (e) PXRD patterns of powder and film on porous α -alumina support of $\text{Cu}_3[\text{Co}(\text{CN})_6]_2 \cdot n\text{H}_2\text{O}$ (where the diffractions originated from α -alumina are marked by asterisks) (f, g) $\text{Cu}_3[\text{Co}(\text{CN})_6]_2 \cdot n\text{H}_2\text{O}$ film on ITO and non-woven fabrics substrates, respectively

The proton conduction was investigated for both powdered pellet sample and the film of $\text{Cu}_3[\text{Co}(\text{CN})_6]_2 \cdot n\text{H}_2\text{O}$ on the porous α -alumina substrate. The relative humidity (RH) was tuned by means of controlling the concentration of salt in water. The real (Z') and the imaginary (Z'') parts of the impedances at selected temperatures are shown in **Fig. 2a** for the $\text{Cu}_3[\text{Co}(\text{CN})_6]_2 \cdot n\text{H}_2\text{O}$ film on the porous α -alumina substrate under 100% RH. The semicircle in the high-frequency regime deals with bulk and grain boundary resistances, whereas the tail at low frequency corresponds to the mobile ions that are blocked by the electrode-electrolyte interface. The conductivity (σ) was obtained by fitting the semicircle in the Z'' vs. Z' plot, and the $\sigma = 1.8 \times 10^{-7} \text{ S cm}^{-1}$ at 20 °C (293 K) under 100% RH. The proton conductivity is not high, but comparable to some MOFs-based proton conductors.¹⁵ As the temperature was increased, the diameter of the semicircle in the Z'' vs. Z' plot becomes small, indicating that the proton conductivity is increased owing to the proton hopping motion thermally activated. The plot of $\ln(\sigma T)$ against $1000/T$ is displayed in **Fig. 2b**, the linear fit was performed to give the activation energies (E_a) of 0.48 eV under 100% RH, and the E_a value is about twice as large as Nafion,¹⁶ but falls within the ranges of MOFs-based proton conductors.^{15, 16}

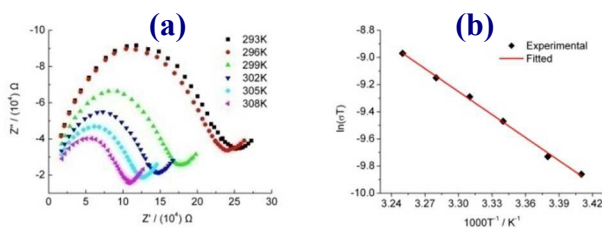
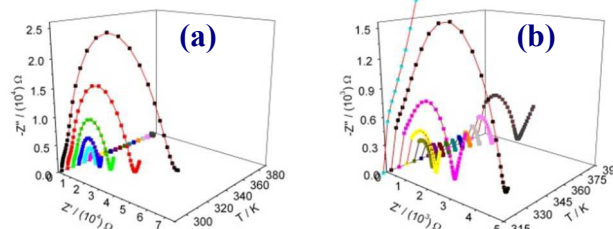


Fig. 2 (a) Plots of Z'' vs Z' at selected temperatures and (b) plot of $\ln(\sigma T)$ vs. $1000/T$ where the red line is the fitted one using Arrhenius equation for $\text{Cu}_3[\text{Co}(\text{CN})_6]_2 \cdot n\text{H}_2\text{O}$ film under 100% RH

The powdered pellet conductivity of $\text{Cu}_3[\text{Co}(\text{CN})_6]_2 \cdot n\text{H}_2\text{O}$ was also investigated, the Z'' vs Z' plots at selected temperatures are shown in **Fig. S2**. The σ value is ca. $2.57 \times 10^{-5} \text{ S cm}^{-1}$ at 303 K under 100% RH, and the activation energy, E_a , for the proton transfer was calculated to be 1.21 eV in line with the linear fit using Arrhenius equation (**Fig. S3**). The different E_a values between the film and pellet samples are probably related to the non-coordination water amount in PBA cavities, which correspond to different proton transport mechanism.¹⁵

In the crystal lattice of $\text{Cu}_3[\text{Co}(\text{CN})_6]_2 \cdot n\text{H}_2\text{O}$, the cyanide ligands bridge linearly two octahedral Cu^{2+} and Co^{3+} ions to create a simple cubic topology. The one third of their octahedral $[\text{Co}(\text{CN})_6]$ units are randomly vacant to yield charge balance, generating six bare-metal sites per formula unit (eight per unit cell) while retaining the simple cubic structure. In the hydrated parent phases, water molecules complete the coordination spheres of the Cu^{2+} ions that surround the vacancy sites, with unbound water filling the remaining pore volume.¹⁷ These water molecules, both coordinated and non-coordinated, are the proton-carrier sources and the hydrogen-bonded networks formed construct proton conduction pathways. The proton transport between the relatively stationary host anions (or proton acceptors) is termed the Grotthuss or free-proton mechanism,¹⁸ otherwise the proton transport by any the other species is termed the vehicle mechanism, which are usually restricted to materials with open structures (channels, layers) to allow passage of the large ions and molecules.³ The Grotthuss mechanism shows lower activation energy of proton transport with respect to the vehicle mechanism.¹⁵ In the lattice of $\text{Cu}_3[\text{Co}(\text{CN})_6]_2 \cdot n\text{H}_2\text{O}$, the protons transfer occurred via both the coordinated (stationary hosts) and non-coordinated water molecules, namely, the Grotthuss and the vehicle mechanisms.

In a proton conductor with water molecules as proton-carrier sources, its proton conductivity is highly correlated with water contents in lattice.¹⁹ The powdered pellet sample impedances of $\text{Cu}_3[\text{Co}(\text{CN})_6]_2 \cdot n\text{H}_2\text{O}$ were further investigated in the temperature range of 293–383 K and under the N_2 atmosphere; the corresponding plots of Z'' vs Z' are displayed in **Figs. 3a** and **3b**, where the diameter of semicircle becomes small with rising temperature in the range of 293–350 K, while increases again above 350 K, indicating that as temperature rises the proton conduction increases below 350 K whereas decreases above 350 K. The proton conductivity was calculated by fitting the semicircle in the $-Z''$ vs. Z' plot at the selected temperature, as shown in **Fig. 3c**, the σ value reaches the maximum ca. 355 K. This situation is due to the proton-carrier sources decreasing with the non-coordinated water molecules releasing, which is confirmed by TG measurement. As shown in **Fig. 3d**, the non-coordinated water molecules can be removed below 400 K, and the maximum of mass losing rate occurs close to 370 K. This observation demonstrated the existence of the inherent water-assisted proton conduction in the coordination framework of $\text{Cu}_3[\text{Co}(\text{CN})_6]_2 \cdot n\text{H}_2\text{O}$,²⁰ namely, the proton transfer undergoes through the hydrogen-bonded networks formed in the crystal lattice.



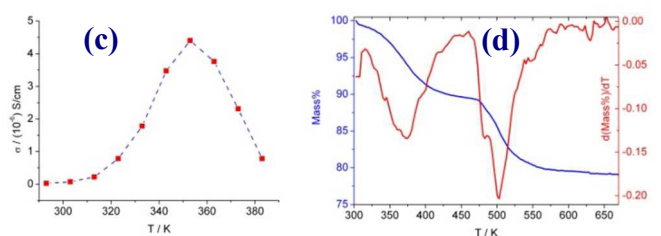


Fig. 3(a, b) Plots of Z'' vs. Z' at selected temperatures for powdered pellet sample of $\text{Cu}_3[\text{Co}(\text{CN})_6]_2 \cdot n\text{H}_2\text{O}$ under N_2 atmosphere. (c) Temperature dependent proton conductivity (d) TG and its first derivative curve of $\text{Cu}_3[\text{Co}(\text{CN})_6]_2 \cdot n\text{H}_2\text{O}$

Prussian blue (PB) and its analogues (PBAs) have attracted evergreen interests of researches in the fields of optical,²¹ electrochromic,²² magnetic,²³⁻²⁵ magneto-optical properties²⁶ as well as biosensor,^{27,28} gas absorption and separation^{13,14} due to their excellent physical and chemical properties. However, the proton conduction of PB and PBAs has received quite little attention.²⁹ On the other hand, recently, there are lots of publications on the study of proton conduction for the MOFs or coordination polymers. To the best of our knowledge, our presentation is the first report on the proton conduction study of PBAs film. Beyond this, the large majority of MOFs are constructed from carboxylates and transition metal ions via weak coordinate bonds, belonging to the salts formed from a weak acid and a weak base, thus, most of MOFs are not water stable,¹¹ although some highly robust MOF materials have emerged recently as well as a few porous coordination compounds are capable of withstanding such strong acidic conditions.³⁰

Conclusions

In summary, we have successfully fabricated the integrated, highly crystalline and water stable PBA film on the porous $\alpha\text{-Al}_2\text{O}_3$, the ITO and the flexible non-woven fabrics substrates, respectively, using the layer-by-layer self-assembly strategy. We also investigated the proton conductivity of both powdered pellet and the film on the porous $\alpha\text{-Al}_2\text{O}_3$ substrate, to demonstrate that PBAs may be the promising proton conducting materials. Our study will shed a light on the practical applications of water stable MOFs-based proton conductors in various devices, such as electrochromatic device, sensor and fuel cell.³¹

This work was supported by the National Natural Science Foundation of China (Nos. 91122011, 21271103 and 21176115) and Innovative Research Team Program by the Ministry of Education of China (No. IRT13070).

Notes and references

^aState Key Laboratory of Materials-Oriented Chemical Engineering, Nanjing Tech University, Nanjing 210009, P. R. China.

^bCollege of Science, Nanjing Tech University, Nanjing 210009, P. R. China.

Email: xmren@njtech.edu.cn (XMR) and wqjin@njtech.edu.cn (WQJ); Fax: +86 25 58139481 and Tel.: +86 25 58139476

† Electronic Supplementary Information (ESI) available: Experimental details and instrumentation. See DOI: 10.1039/c000000x/

- G. A. Voth, *Acc. Chem. Res.* 2006, **39**, 143.
- A. Royant, K. Edman, T. Ursby, E. Pebay-Peyroula, E. M. Landau, R. Neutze, *Nature* 2000, **406**, 645.
- T. Norby, *Solid State Ionics* 1999, **125**, 1.

- C. Laberty-Robert, K. Valle, F. Pereira, C. Sanchez, *Chem. Soc. Rev.* 2011, **40**, 961.
- H. Iwahara, T. Esaka, H. Uchida, N. Maeda, *Solid State Ionics* 1981, **3-4**, 359.
- T. Norby, N. Christiansen, *Solid State Ionics* 1995, **77**, 240.
- D. Umeyama, S. Horike, M. Inukai, S. Kitagawa, *J. Am. Chem. Soc.* 2013, **135**, 11345.
- S. S. Bao, K. Otsubo, J. M. Taylor, Z. Jiang, L. M. Zheng, H. Kitagawa, *J. Am. Chem. Soc.* 2014, **136**, 9292.
- M. Yoon, K. Suh, S. Natarajan, K. Kim, *Angew. Chem. Int. Ed.* 2013, **52**, 2688.
- M. Sadakiyo, T. Yamada, K. Honda, H. Matsui, H. Kitagawa, *J. Am. Chem. Soc.* 2014, **136**, 7701.
- J. M. Taylor, K. W. Dawson, G. K. H. Shimizu, *J. Am. Chem. Soc.* 2013, **135**, 1193.
- X. Y. Dong, R. Wang, J. B. Li, S. Q. Zang, H. W. Hou and T. C. W. Mak, *Chem. Commun.* 2013, **49**, 10590.
- S. S. Kaye, J. R. Long, *J. Am. Chem. Soc.* 2005, **127**, 6506.
- P. K. Thallapally, R. K. Motkuri, C. A. Fernandez, B. P. McGrath, G. S. Behrooz, *Inorg. Chem.* 2010, **49**, 4909.
- A. Shigematsu, T. Yamada, H. Kitagawa, *J. Am. Chem. Soc.* 2011, **133**, 2034.
- M. Sadakiyo, T. Yamada, H. Kitagawa, *J. Am. Chem. Soc.* 2009, **131**, 9906.
- S. H. Ogilvie, S. G. Duyker, P. D. Southon, V. K. Peterson, C. J. Kepert, *Chem. Commun.* 2013, **49**, 9404.
- N. Agmon, *Chem. Phys. Lett.* 1995, **244**, 456.
- A. Mallick, T. Kundu, R. Banerjee, *Chem. Commun.* 2012, **48**, 8829.
- S. S. Nagarkar, S. M. Unni, A. Sharma, S. Kurungot, S. K. Ghosh, *Angew. Chem. Int. Ed.* 2014, **53**, 2638.
- R. Koncki, T. Lenarczuk, S. Glab, *Anal. Chim. Acta* 2000, **424**, 27.
- A. Kraft, M. Rottmann, *Sol. Energy Mater. Sol. Cells* 2009, **93**, 2088.
- T. Mallah, S. Thiebaut, M. Verdager, P. Veillet, *Science* 1993, **262**, 1554.
- O. Sato, T. Iyoda, A. Fujishima, K. Hashimoto, *Science* 1996, **272**, 704.
- G. Maurin-Pasturel, J. Long, Y. Guari, F. Godiard, M.-G. Willinger, C. Guerin, J. Larionova, *Angew. Chem. Int. Ed.* 2014, **53**, 3872.
- S.-i. Ohkoshi, S. Takano, K. Imoto, M. Yoshikiyo, A. Namai and H. Tokoro, *Nat. Photonics* 2014, **8**, 65.
- Z. Y. Chu, Y. N. Zhang, X. L. Dong, W. Q. Jin, N. P. Xu, B. Tieke, *Chem. Commun.* 2010, **20**, 7815.
- Z. Y. Chu, L. Shi, Y. N. Zhang, W. Q. Jin, S. Warren, D. Ward, E. Dempsey, *J. Mater. Chem.* 2012, **22**, 14874.
- S.-i. Ohkoshi, K. Nakagawa, K. Tomono, K. Imoto, Y. Tsunobuchi, H. Tokoro, *J. Am. Chem. Soc.* 2010, **132**, 6620.
- V. G. Ponomareva, K. A. Kovalenko, A. P. Chupakhin, D. N. Dybtsev, E. S. Shutova, V. P. Fedin, *J. Am. Chem. Soc.* 2012, **134**, 15640.
- K.-D. Kreuer, *Chem. Mater.* 1996, **8**, 610.